RJC

RASĀYAN *J. Chem.*
Vol. 12 | No. 3 |1326 - 1339| July - September | 2019
ISSN: 0974-1496 | e-ISSN: 0976-0083 | CODEN: RJCABP
http://www.rasayanjournal.com
http://www.rasayanjournal.co.in

CORROSION RESISTANCE OF *Cissus quadrangularis* EXTRACTS ON METAL IN AGGRESSIVE MEDIUM: GRAVIMETRIC AND SURFACE EXAMINATIONS

R. Anitha[1] and Subramanian Chitra[2,*]

[1]Department of Chemistry, SNS College of Technology, Coimbatore- 641035, Tamilnadu, India
[2]Department of Chemistry, PSGR Krishnammal College for Women,
Coimbatore - 641004, Tamilnadu, India
*E-mail: rajshree1995@rediffmail.com

ABSTRACT

The corrosion resistance of *Cissus quadrangularis* in acid and ethanol medium have been investigated by diverse techniques. It has been noticed that as the concentration (2 to 12v/v %) of *C. quadrangularis* rises the efficiency of the inhibitor also increases. The maximum inhibition efficiencies of 89.45 % and 75.54 % were attained for acid and ethanol extracts respectively. The emergence of a protective layer on the mild steel surface was assessed by electrochemical impedance studies. The influence of the active ingredients in the extracts was examined by GC-MS analysis. The inhibitor adsorption ensued in the protective layer on the surface was analyzed using SEM and AFM.

Keywords: *C. quadrangularis, GC-MS,* Electrochemical Techniques, Adsorption Isotherm, SEM, AFM

INTRODUCTION

Mild steel is the dominant metal that has wide application in industries. It is highly affected due to corrosion because of the usage of acid solutions in industries for descaling, acid pickling, petrochemical processes etc.[1,2] The metal corrosion in the corrosive medium is a complex problem world wide. To alleviate corrosion various proactive techniques such as improvement in materials, anodic/cathodic protection, coatings, modification of materials and corrosion inhibitors are used[3,4]. Among these techniques, corrosion inhibitors play a predominant role in protecting the metal against corrosion, particularly in acid medium. An organic compound functions as an inhibitor having hetero atoms, aromatic rings, conjugated double (or) triple bond, π-electrons in their structure[5]. In general, synthetic inhibitors are effective to abate corrosion but due to adverse effects of these inhibitors researchers are focussing towards non-toxic, cheap, biodegradable, readily existing green inhibitors[6]. A wide number of scientific research have been carried out to analyze the anti-corrosive property of various plant extracts on corrosion of metals, to discuss a few, *Cymbopogan Citratus*[7], *Phyllanthus amarus*[8], *Cascabela Thevetia*[9], *Grewa Venusta*[10], Arecanut husk[11]. In our current research, we focussed on the easily available plant *Cissus quadrangularis (CQ).* This plant originates under the type of vitaceae family with more traditional medicinal values. It is also termed as veld grape. CQ belongs to Srilanka and it is broadly spread in South East Asia, Arabic countries and Africa[12]. It possesses activities like gastro protective, anti-inflammatory anti-microbial, anti-tumor, etc. The literature evidenced the presence of amyrines, phenols, tannins etc., in CQ.

EXPERIMENTAL

Preparation of Inhibitor and Metal Specimen

Cissus quadrangularis were collected in the nearby vegetable market, washed thoroughly with water to eradicate impurities, dried. After the completion of drying it was powdered to obtain fine particles. About 1g of the grounded sample was heated in 100 ml of 0.5 M H_2SO_4 (acid extract) / 100 ml of ethanol (ethanol extract) in a round-bottomed flask for 3 hours. The resultant green extracts [acid (CQAE)] and [ethanol (CQEE)] extracts were cooled at room temperature and filtered using Whatman filter paper.

http://dx.doi.org/10.31788/RJC.2019.1235195

CrossMark

These extracts were stored in a refrigerator and utilized as an inhibitor for further analysis. Specimens were cut into rectangular sheets of specific dimensions 3 cm x 1 cm x 0.1 cm polished using emery paper, wiped with acetone and plates were kept in a moisture-free desiccator.

Spectral Analysis

FT-IR Spectroscopy and GC-MS Analysis

The active functional group existing in CQAE and CQEE extracts were recorded by Shimadzu IR affinity instruments. The bio phyto constituents present in the extracts were examined by Perkin Elmer Clasus 60 GC-MS instrument.

Gravimetric Measurements

After completion of pre cleaning process of metal coupons, the initial weight of the coupon was taken, suspended in a solution containing blank (un inhibited solution) and inhibited solutions (CQAE and CQEE) of concentrations (2, 4, 6 ,8, 10, 12, 14 v/v %) in a 100 ml beaker. After a specified time of 3 hours, the mild steel specimens were taken out, cleansed with water, dehydrated using warm air and reweighed. The loss in weight was calculated from the preliminary and final weights of the metal specimen. Differences in weight were used to evaluate inhibition efficiency (IE %) and corrosion rate (CR) based on the formula[13],

$$\text{Inhibition efficiency (\% IE)} = \frac{W_{bl} - W_{in}}{W_{bl}} \text{x}100 \quad (1)$$

$$\text{Corrosion rate } (C_{rate}) = \frac{534 \text{ x loss in weight (g)}}{\text{Density (g/cm}^3\text{) x Area (cm) x Time (hr)}} \quad (2)$$

Where, W_{bl} – blank weight loss, W_{in} - inhibitor weight loss. The above-mentioned procedure was followed to scrutinize the impact of temperature on corrosion behavior. Gravimetric measurements were done in the range of temperature (313 - 333K) and various parameters such as enthalpy and entropy, activation energy (E_a), were determined by using the formula as reported in the previous literature[14].

Electrochemical Techniques

The measurements based on electrochemical techniques such as impedance and polarisation studies for inhibited and uninhibited solutions were recorded using IVIUM compact stat Potentiostat/ Galvanostat. A traditional three-electrode cell assembly was utilized with the auxiliary electrode as platinum foil, saturated calomel electrode as reference and working electrode (mild steel specimen). Charge transfer resistance (R_{ct}) and double-layer capacitance (C_{dl}) from the impedance graphs were determined [15,16]. Polarisation measurement was conducted in the range of -200 mV to +200 mV to get a smooth polarisation curve and scan rate was fixed to 1mV/sec. From this data I_{corr} (corrosion current), E_{corr} (corrosion potential) and Tafel slopes (b_a and b_c) were determined with and without the addition of the inhibitors. The inhibition efficacy was calculated using equation [17],

$$\text{Inhibition efficiency}(\%\text{IE}) = \frac{R_{ct(in)} - R_{ct(bl)}}{R_{ct(in)}} \text{x}100 \quad (3)$$

$$\text{Inhibition efficiency}(\%\text{IE}) = \frac{I_{corr(bl)} - I_{corr(in)}}{I_{corr(bl)}} \text{x}100 \quad (4)$$

Surface Morphological Studies

Scanning Electron Microscope

The metal coupons were suspended in the uninhibited and inhibited solution for 3 hours. Then they were detached from the beaker, cleansed with water, dried and analyzed using biomedical research microscope (Mumbai, India).

Atomic Force Microscopy

A multimode scanning probe microscope (NTMDT, NTEGRA prima, Russia) was utilized to examine the morphological analysis on the surface of the metal samples immersed in a solution containing inhibitor and without inhibitor for a specified time of 3 hours. Then it was taken out, washed, dried and analyzed.

RESULTS AND DISCUSSION

FT-IR Spectra

CQAE and CQEE FT-IR spectra was portrayed in Fig.-1. Band at 3621 cm^{-1}, 1738 cm^{-1}, 1364 cm^{-1} correspond to >OH, >C=O, >CH vibrations in CQAE. The absorption bands of CQEE at 3700 cm^{-1}, 1715 cm^{-1}, 1410 cm^{-1} and 715 cm^{-1} are related to >OH, >C=O, >C=C, >C-H vibrations.

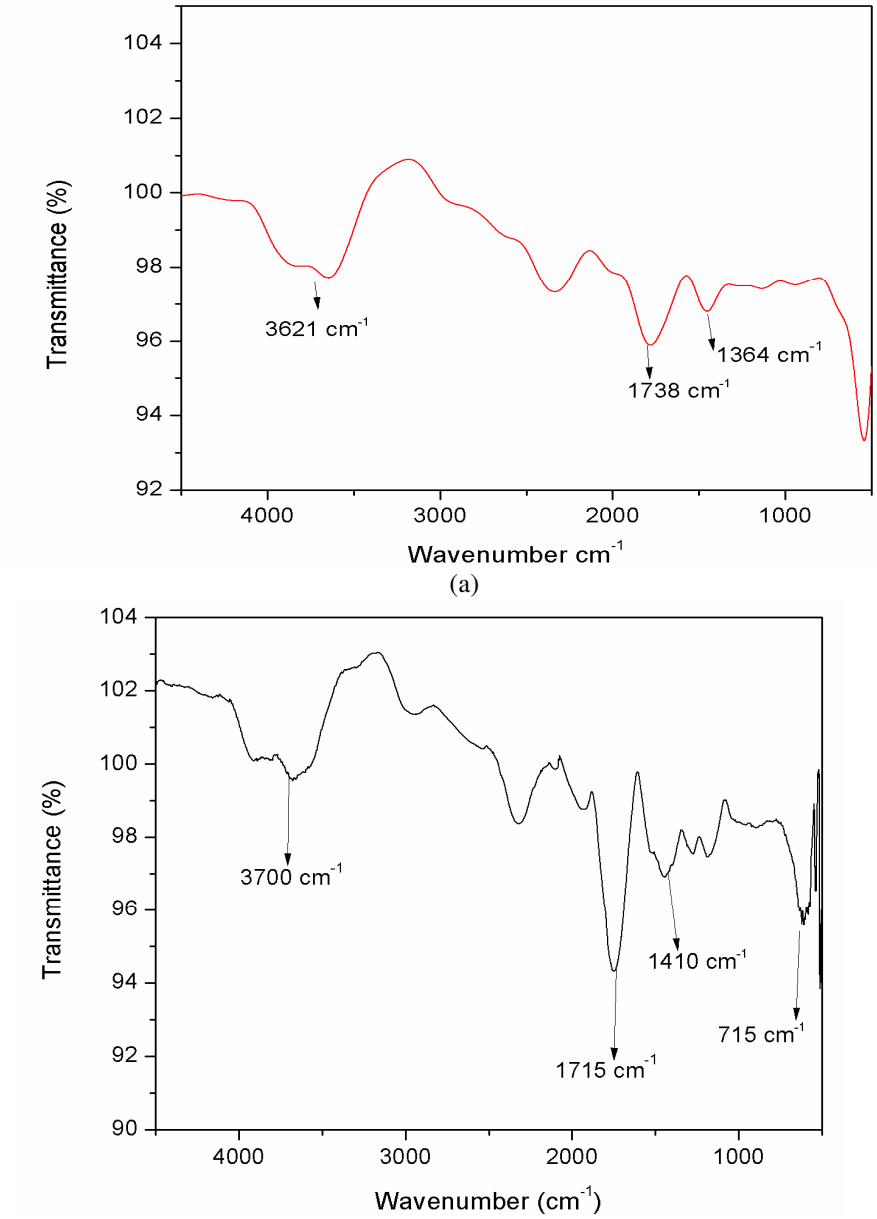

Fig.-1: IR Spectra of (a) CQAE (b) CQEE

Gas Chromatography-Mass Spectroscopy Analysis (GC- MS)

GC-MS Chromatogram of *Cissus quadrangularis* (acid and ethanol extracts) are represented in Fig.-2. The mass spectra of disiloxane, 1, 3-diethoxy-1, 1, 3, 3-tetramethyl and ethyl oleate are shown in Fig.-3. With the help of the NIST library, the structure of the compound existing in the extracts were analyzed. Based on the peak area, predominant 6 compounds were identified for CQAE and 4 compounds for CQEE. The structure of the compounds is represented in Fig.-4.

The compounds are (a) disiloxane,1,3-diethoxy-1,1,3,3-tetramethyl (b) cyclotetrasiloxane, octamethyl- (c) linoleic acid ethyl ester (d) 4-hydroxy chalcone (e) benzo (a) heptalene-7, 9-dione, 5, 6-dihydro-1, 2, 3,

10-tetramethoxy (f) stigmasta-3,5 diene in CQAE. Predominant compounds of CQEE are (a.1) ethyl oleate (b.1) 9-octadecenoicacid pentyl ester (c.1) 7, 11, 15 - trimethyl-3-methylidenehexadec-1-ene (d.1) n- hexadecanoic acid.

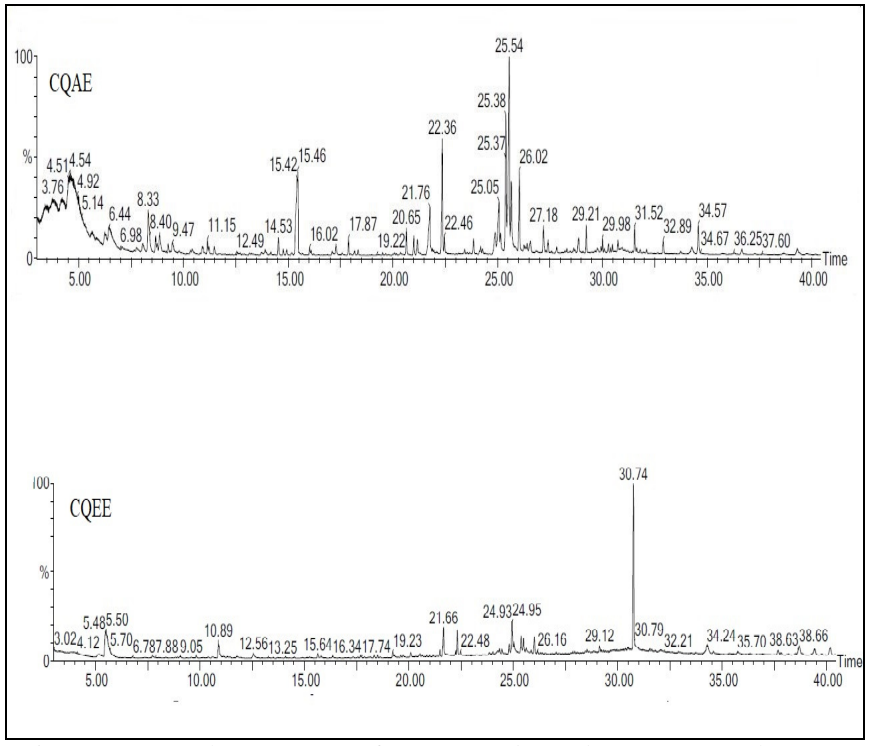

Fig.-2: GC-MS Chromatogram of *Cissus quadrangularis* (CQAE and CQEE)

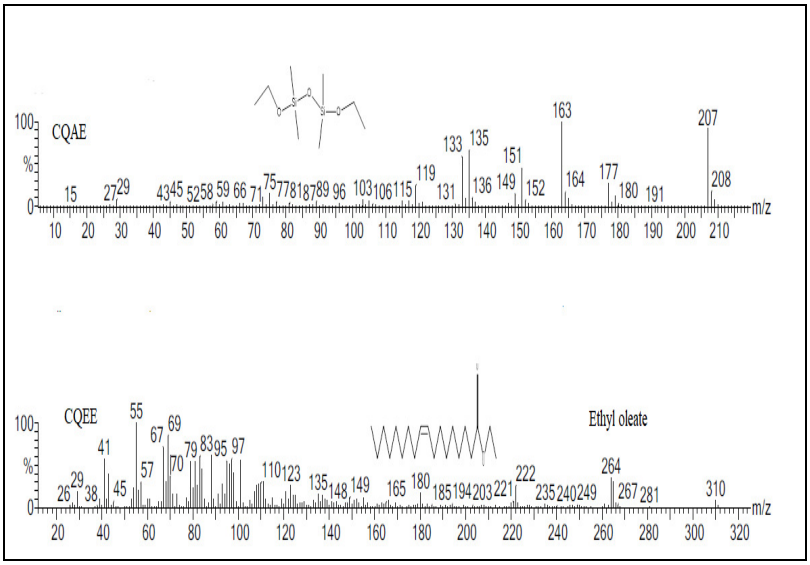

Fig.-3: Mass Spectra of Disiloxane, 1, 3-diethoxy-1, 1, 3, 3-tetramethyl and ethyl oleate

Out of these, in CQAE disiloxane,1, 3-diethoxy-1,1,3,3-tetramethyl relates to the maximum peak area of 6.320 % and the probability of matching is 77.7%, comprising of electronegative atoms such as oxygen. In CQEE, the major component is ethyl oleate of peak area 6.041 % containing oxygen atoms.

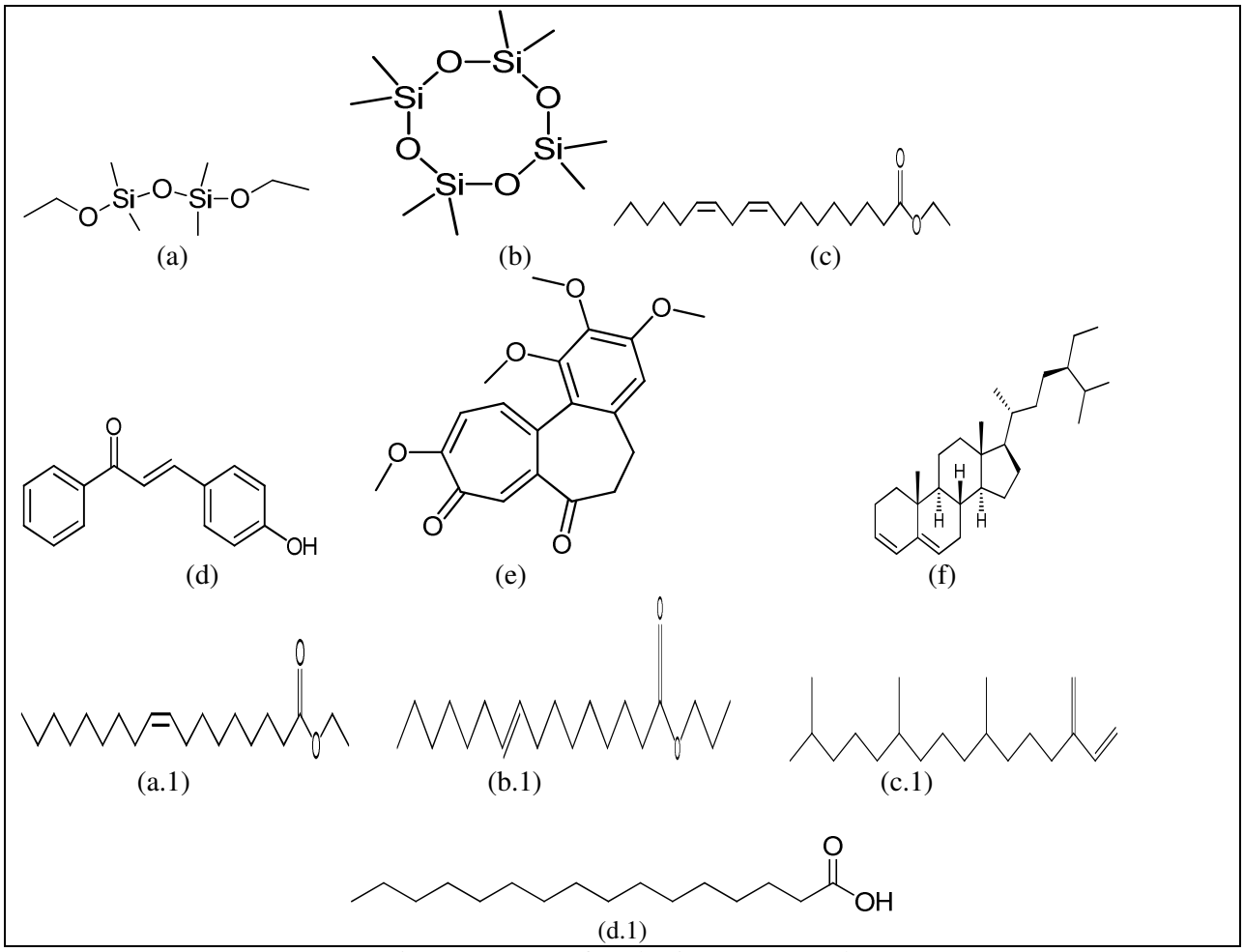

Fig.-4: Structure of Predominant Compounds

Gravimetric Measurements

The efficiency of the inhibitor at diverse concentrations (2 – 12 v/v %) on mild steel in 0.5 M sulphuric acid was analyzed and results are accessible in Table-1. It denotes that as the concentration CQAE and CQEE increased the efficiency also increased whereas the corrosion rate reduced.

Table-1: Inhibition Efficiencies at Different Concentrations of CQAE and CQEE on Mild Steel in 0.5M H_2SO_4 attained by Mass Loss Measurements at Room Temperature

Name of the Inhibitor	Conc. (v/v %)	IE (%)	Surface Coverage(θ)	CR (mpy)
Blank	-	-	-	7682.246
CQAE	2	76.82	0.7682	1780.85
	4	81.52	0.8152	1420.00
	6	86.88	0.8688	1007.94
	8	87.23	0.8723	981.12
	10	88.29	0.8829	899.69
	12	89.45	0.8945	810.45
	14	89.48	0.8948	810.11
CQEE	2	47.71	0.4771	4017.16
	4	50.49	0.5049	3803.57
	6	56.02	0.5602	3378.35

	8	67.16	0.6716	2523.03
	10	71.05	0.7105	2224.11
	12	75.54	0.7554	1879.35
	14	75.59	0.7559	1855.12

Beyond 12v/v % even though the concentration has increased the efficiency attained a saturation level indicating the optimum concentration. In CQAE, even at a minimum concentration of 2 v/v % the efficiency reached to 76.82 % whereas for CQEE at 2 v/v % efficiency was 47.71 %. Increase of concentration of CQAE and CQEE increased the adsorption of the organic moieties on the metal surface in turn surface coverage increased thus protecting the metal from immediate aggressiveness of acid. Comparing CQAE and CQEE, increased efficacy of CQAE could be due to the existence of more organic compounds comprising hetero atoms and π-electrons, high molecular weight compounds compared to CQEE thus providing more adsorption sites.

Role of Temperature on IE

The role of temperature on the corrosion process occurring at the metal surface with and without the influence of the inhibitors (CQAE and CQEE) in 0.5M sulphuric acid were evaluated in the temperature range 313 - 333K.

Table-2: Inhibition Efficiencies of CQAE and CQEE Inhibitors on Mild Steel in 0.5M Sulphuric Acid at Higher Temperatures

Inhibitor	Conc. (v/v %)	Temperature							
		303		313		323		333	
		IE%	CR(mpy)	IE%	CR(mpy)	IE%	CR(mpy)	IE%	CR(mpy)
Blank	-	-	7705.17	-	10666.10	-	16822.04	-	29997.04
CQAE	2	75.8	588.21	60.10	4125.22	42.98	9548.22	35.65	18999.22
	6	84.89	380.96	74.34	2588.42	63.87	5734.67	55.67	12876.87
	12	89.08	245.12	75.67	2521.34	77.04	2410.77	64.5	10674.87
CQEE	2	47.86	4017.16	45.06	5860.43	43.13	9567.45	39.90	18028.95
	6	68.33	3377.87	59.13	4359.48	55.47	7490.12	43.72	16882.02
	12	75.34	1900.03	61.21	4137.12	59.32	6843.51	53.66	13900.60

It can be noticed from Table-2 that as the temperature is inflated there is a rise in corrosion rate resulting in desorption of the molecules exposing more surface area to corrosion[18]. Influence of temperature on inhibitor ability was interrelated by Arrhenius and Transition state equation. In Fig.-5 a linear graph was obtained for Arrhenius and Transition plots. E_a values were calculated from the slope and it is tabulated in Table-3. Datas for ΔH^o and ΔS^o were evaluated from the linear plot of the slope. It is apparent from Table-3 that E_a values of the inhibitors (70.97 and 54.32 kJ mol^{-1}) are higher than blank (37.87 kJ mol^{-1}) which intimates that in presence of inhibitors a protective barrier is formed thus impeding corrosion. Positive ΔH^o (69.33 and 51.31 kJ mol^{-1}) suggests endothermic nature intimates that in presence of inhibitor the dissolution of metal is retarded[19]. Negative values of ΔS^o (-18.25, -11.12 J $mol^{-1}K^{-1}$) specifies a decrease in disorderness occurs from reactant to activated complex[20, 21].

Table-3: Activation Parameters of Dissolution of Metal in the Corrosive Medium in the Non-existence and Presence of Inhibitors

Inhibitor	E_a kJ mol^{-1}	ΔH^o kJ mol^{-1}	ΔS^o J $mol^{-1}K^{-1}$	$+\Delta G^o$ (kJ mol^{-1})			
				303	313	323	333
Blank	37.87	35.24	-46.52	12.31	13.37	14.4	15.5
CQAE	70.97	69.33	-18.25	5.66	5.97	6.35	6.80
CQEE	54.32	51.31	-11.12	4.51	4.75	5.38	5.66

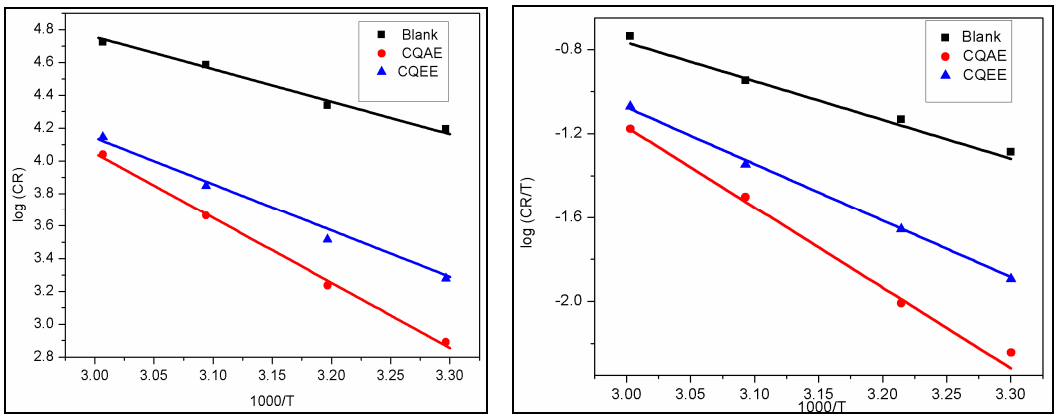

(a) (b)

Fig.-5: (a) Arrhenius Plot (b) Transition Plots of CQAE and CQEE

Positive ΔG^o values stipulate the instability of the activated complex. A straight line plot is attained for $\ln K_{ads}$ vs 1/T having a slope (ΔH^o_{ads} / R) and intercept [(ΔS^o_{ads}/R) +ln (1/55.5)] and it is represented in Fig.-6.

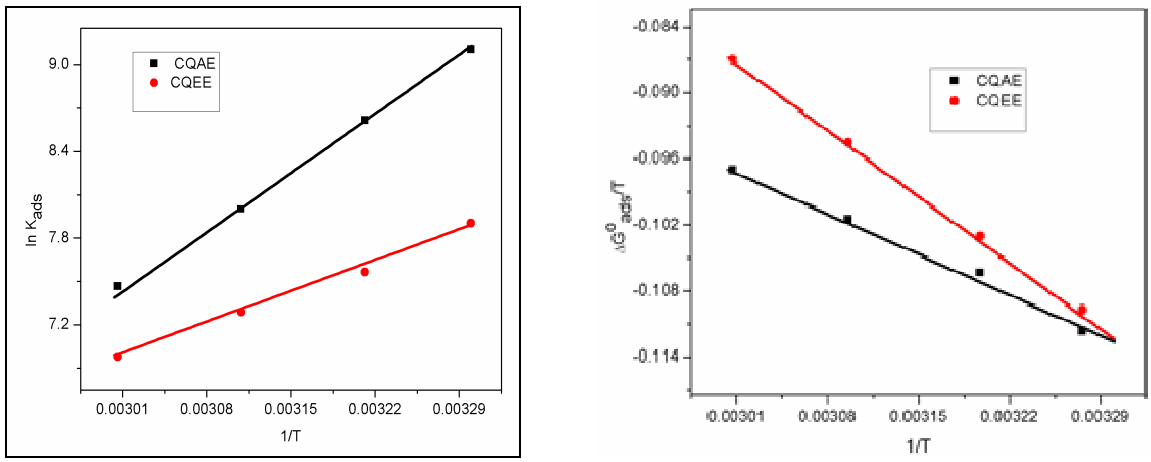

(a) (b)

Fig.-6: (a) Van't Hoff (b) Gibbs-Helmholtz Plots for Mild Steel in 0.5M H_2SO_4 in presence of Acid and Ethanol Extracts of CQ

From Table-4 it is evident that ΔH^o is negative (-25.29, -22.68 kJ mol^{-1}) indicates exothermic adsorption process. The value of ΔG^o for CQAE and CQEE are around -27.89 to -32.77 kJ mol^{-1} suggesting a mixed mode of adsorption predominantly physisorption.

Adsorption isotherm

The corrosion inhibition behavior on the metal surface is highly based on adsorption process[22]. The mass loss measurements provides θ values with varying concentrations of CQAE and CQEE. The experimental data were fitted for various adsorption isotherms like Frumkin, Freundlich, Langmuir, Flory-Huggins and Temkin isotherms. The relation between inhibitor concentration (C_{in}) and surface coverage (θ) is given by the equation,

$$\frac{C_{in}}{\theta} = \frac{1}{K_{ads}} + C_{in} \qquad (5)$$

Table-4: Van't Hoff Equation and Gibbs Helmholtz Equation Derived from Thermodynamic Parameters

Inhibitor	Van't Hoff equation		Gibbs-Helmholtz equation	ΔG°_{ads} kJ mol^{-1}			
	ΔH°_{ads} kJ mol^{-1}	ΔS°_{ads} kJ mol^{-1}	ΔH°_{ads} kJ mol^{-1}	303 K	313 K	323 K	333 K
CQAE	-25.29	-0.095	-25.29	-32.77	-32.46	-29.35	-28.93
CQEE	-22.68	-0.092	-22.68	-30.33	-28.67	-28.47	-27.89

Linear plots were attained for C/θ vs C and it is shown in Fig.-7. Langmuir adsorption isotherm fitted well.

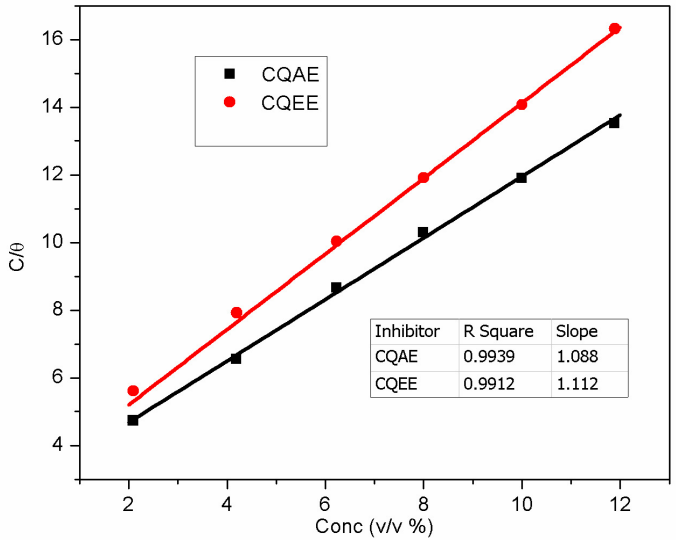

Fig.-7: Langmuir Adsorption Isotherm Plot of Acid and Ethanol Extracts of *C.quadrangularis* on Mild Steel

Moreover, K_{ads} value is acquired from the intercept of the graph and it is tabulated in Table-5 and ΔG^{o}_{ads} can be calculated by using the equation,

$$\Delta G^{o}_{ads} = -RT\ln(55.5K) \qquad (6)$$

Since, ΔG^{o}_{ads} value is negative which specifies spontaneous adsorption of CQAE and CQEE on the metal surface via physisorption mechanism[23]. The calculated values of ΔG^{o} (-30.17, -30.26 kJ mol^{-1}) implies mixed-mode predominantly physisorption.

Table-5: Langmuir Adsorption Parameters for CQAE and CQEE

Inhibitor	R^2	Slope	K (mol lt^{-1})	$-\Delta G^{\circ}_{ads}$ (kJ mol^{-1})
CQAE	0.9939	1.08	296.6	30.17
CQEE	0.9912	1.11	286.6	30.26

Electrochemical Impedance Spectroscopy

Impedance spectroscopy helps to understand the kinetics and surface characteristics of the metal. The nyquist plot is the representation of reaction occurring at the surface[24]. Fig.-8 demonstrates Nyquist plots of selected concentrations of CQAE and CQEE. On analyzing Table- 6 the R_{ct} value increases as the concentration of the inhibitors (CQAE and CQEE) increases proving the presence of a protective layer on

the metal surface. Reduction in C_{dl} with the rise in inhibitor concentration is observed owing to increase in adsorption, which contributes more surface coverage, in turn, enhancing the inhibition efficiency[25]. This attributed to the progress in the thickness of the double layer due to the presence of adsorbed molecules of the extracts thus impeding mild steel corrosion /electrolyte interface. Variation in C_{dl} values indicates that water molecules are altered by CQAE and CQEE.

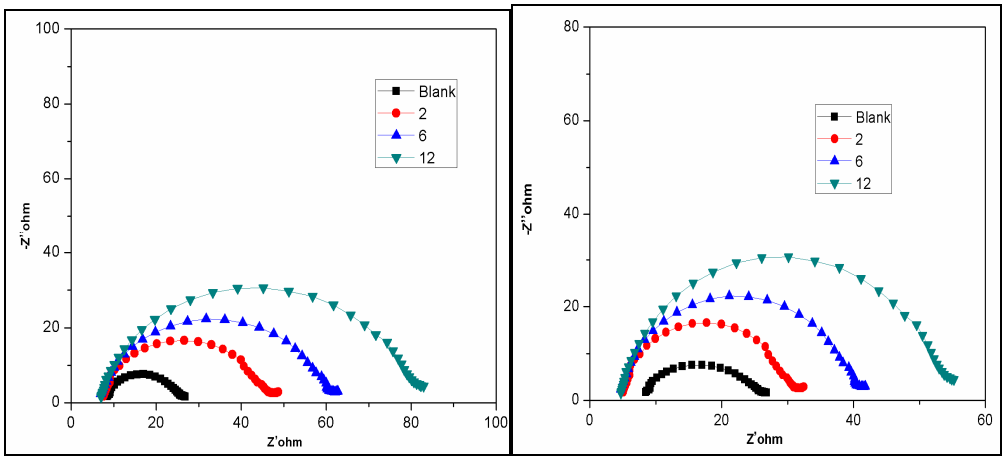

(a) (b)

Fig.-8: Nyquist Plots of (a) CQAE (b) CQEE

Table-6: AC-Impedance Parameters for Mild Steel Corrosion in 0.5M H_2SO_4 in the Absence and Presence of Selected Concentrations of Acid and Ethanol Extracts of *C.quadrangularis*

Name of the inhibitor	Conc. (v/v %)	R_{ct} (ohm cm^2)	C_{dl} ($\mu F/cm^2$)	IE (%)
Blank	-	17	61	-
CQAE	2	42	56.5	59.5
	6	57	40.1	70
	12	77	37.9	78
CQEE	2	25	42.3	32
	6	40	35.1	57.5
	12	52	21.2	67.3

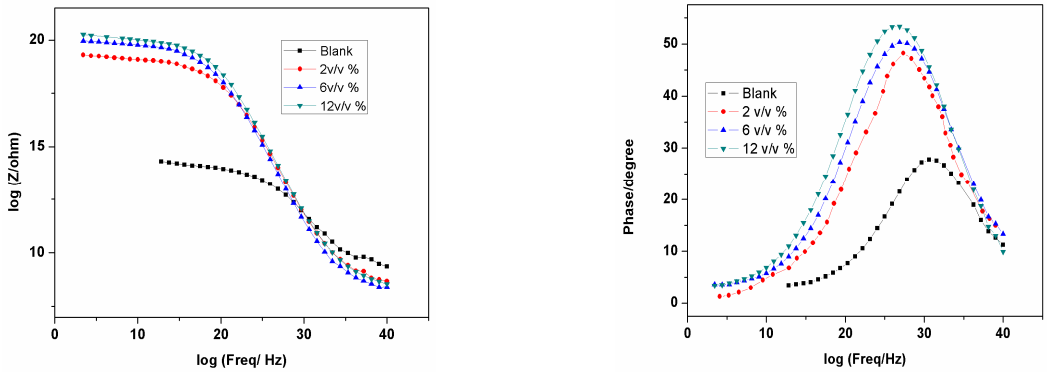

(a)

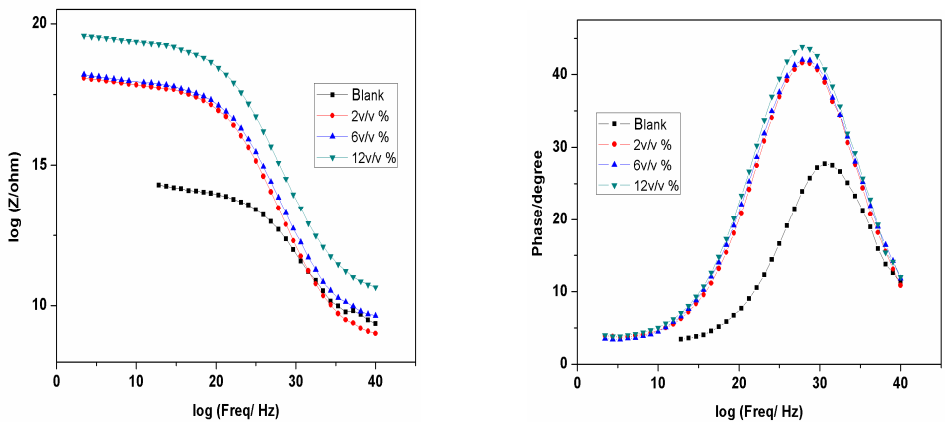

(b)

Fig.-9: Bode Plots of (a) CQAE (b) CQEE

Bode plots of corrosion on metal in non-existence and presence of inhibitors of concentrations (2, 6 and 12v/v %) in 0.5M H_2SO_4 are illustrated in Fig.-9. It is inferred from the plot that as the concentration of CQAE and CQEE increases phase angle increases which specifies the reduction in surface inhomogeneity. Also, a resistance towards corrosion rises as the concentration rises suggested reduced metal dissolution [26].

Potentiodynamic Polarisation Techniques

Emblematic Tafel plots for mild steel in 0.5M H_2SO_4 of varying concentrations are depicted in Fig.-10. It is apparent from the Fig.-10 that as the concentration of CQAE and CQEE increases the corrosion potential (E_{corr}) slightly shifted proposing mixed behavior of the inhibitor with slightly cathodic.

As per literature, E_{corr} value less than 85mV indicates the mixed nature of the inhibitor with reference to that the maximum displacement in our current research was 70mV proving the mixed behavior[27,28]. The parameters such as b_a, b_c, I_{corr}, E_{corr} and inhibition efficiency are in Table-7. It can be grasped from Table-7, that I_{corr} value decreases as the concentration of *C. quadrangularis* increases evidencing the adsorption process takes place thus impeding corrosion.

.

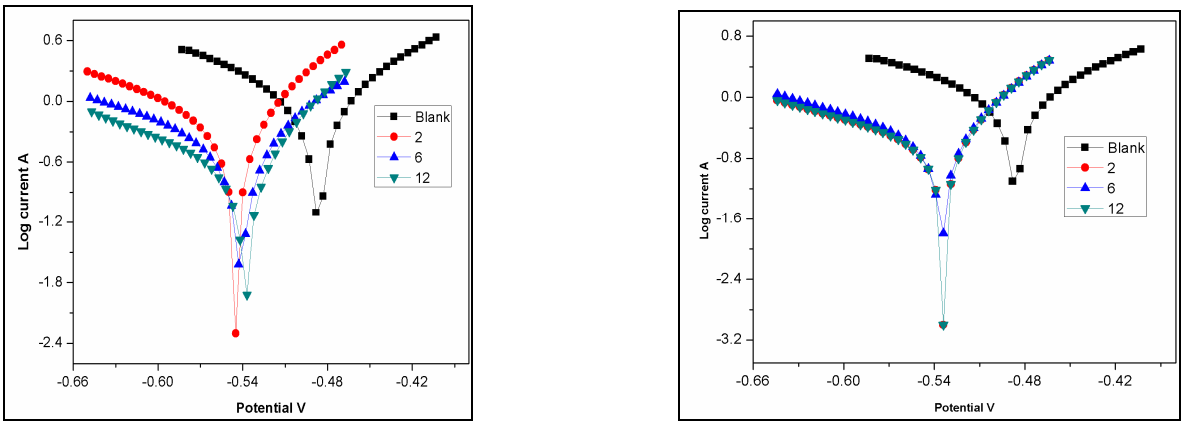

(a) (b)

Fig.-10: Tafel Curves for Mild Steel in 0.5 M H_2SO_4 Solution in the Absence and Presence of Selected Concentrations of (a) CQAE (b) CQEE

Scanning Electron Microscope (SEM)

On analyzing SEM visuals of blank, CQAE and CQEE at an optimum concentration of 12v/v % in Fig.-11 the morphology of the metal surface can be visualized. Fig.-11a (blank) indicates cracks, pits and

rough surface owing to the violent attack of acid. The presence of inhibitors (CQAE and CQEE) in Fig.-11b and c represents the formation of the protective layer thus reducing corrosion, with respect to vibrant interaction of the inhibitor molecules on the metal surface

Table -7: Corrosion Parameters for Metal in 0.5M H_2SO_4 of Acid and Ethanol Extracts of *C.quadrangularis* by Potentiodynamic Polarization Method

Inhibitor	Conc. (v/v %)	Tafel Slopes (mV/dec)		$-E_{corr}$ (mV)	I_{corr} ($\mu A/cm^2$)	IE (%)
		b_a	b_c			
Blank	-	62	91	490	520	-
CQAE	2	80	175	538	215	58.6
	6	71	170	537	155	70.1
	12	59	161	536	113	78.2
CQEE	2	70	168	545	340	34.6
	6	61	152	540	216	58.3
	12	42	132	538	180	65.4

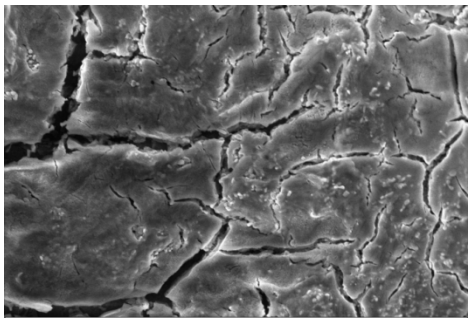

(a)

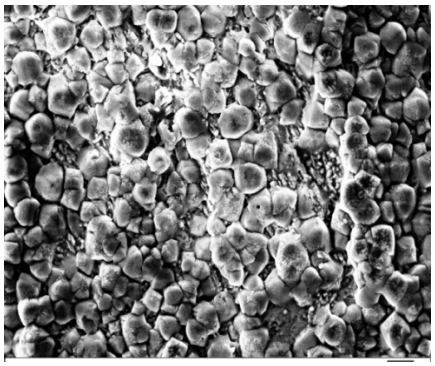

(b)

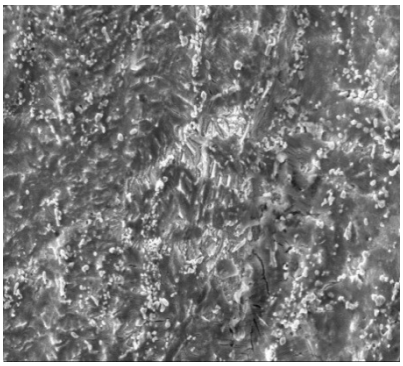

(c)

Fig.-11: SEM Visuals of (a) Blank (b) CQAE (c) CQEE

Atomic Force Microscopy

AFM is a new technique to analyze the characteristics of the defensive layer on the metal surface[29]. A 3D and 2D AFM images of metal specimens in 0.5M H_2SO_4 are represented in Fig.-12. AFM visuals of metal in the presence of inhibitors (CQAE and CQEE) at an optimum concentration (12v/v %) are portrayed in Fig.-12 b and c. It can be viewed from the images that a blank specimen image displays more roughness in comparison with CQAE and CQEE images. Average roughness is calculated for the specimen in acid solution and it is found to be 180.17 nm whereas for CQAE and CQEE are 95.62 nm and 106.12 nm respectively. The reduction in average roughness validates the formation of the protective layer due to CQAE and CQEE[30].

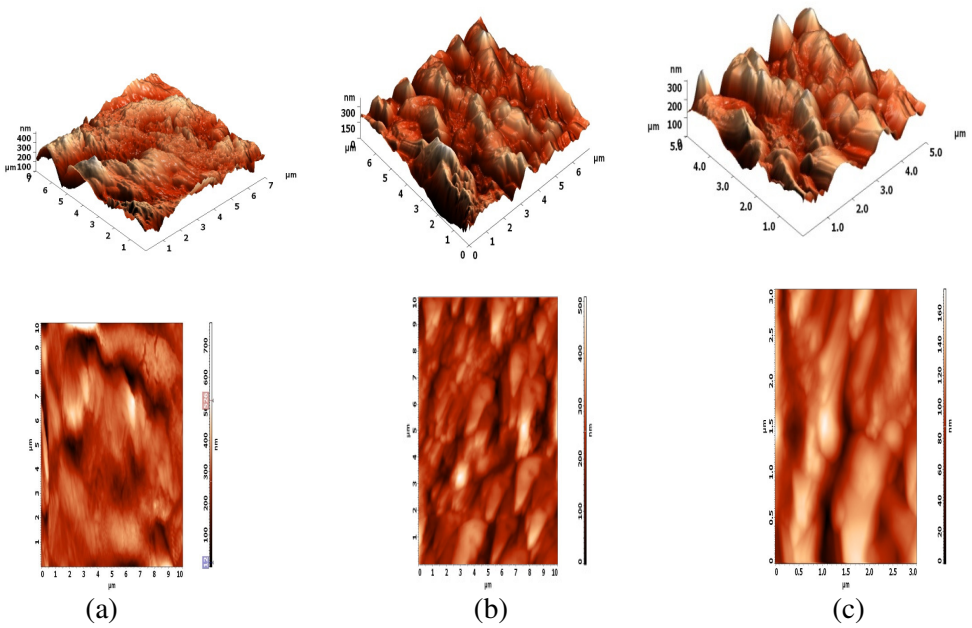

Fig.-12: AFM 3D and 2D Images of (a) Blank (b) CQAE (c) CQEE

Proposed Mechanism of Inhibition

In acidic medium, mild steel surface acquires negatively charge owing to the influence of adsorbed SO_4^{2-} ions on the mild steel surface[31].

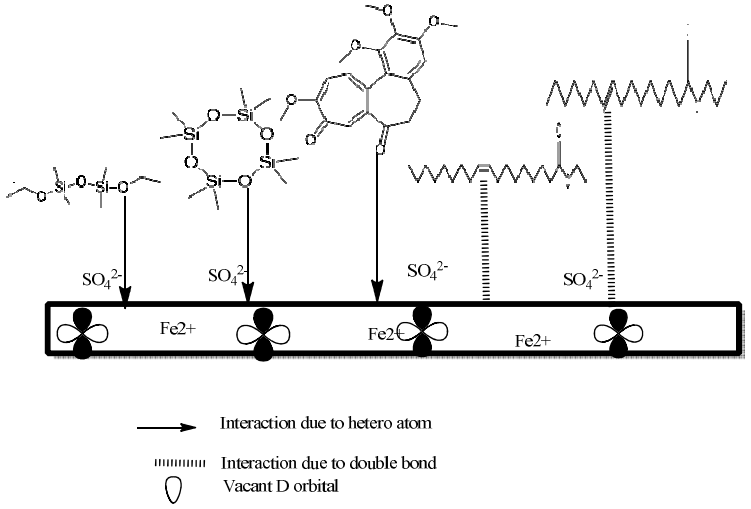

Fig.-13: Schematic Representation for the Proposed Mechanism of Inhibition

In a sulphuric acid medium, the oxygen atoms present in the major predominant compounds such as disiloxane, 1, 3-diethoxy-1, 1, 3, 3-tetramethyl, ethyl oleate gets protonated because of their high electron density hence the inhibitor acquires a positive charge. Due to the electrostatic attraction between negatively charged mild steel surface and inhibitor with positive charge interacts and adsorption takes place. The protonated inhibitor easily adsorbed on cathodic site of the metal thus decreasing the evolution of hydrogen[32]. This adsorption outcome resulted in the development of the protective layer at the mild

steel/electrolyte interface. A coordinate bond exists between the lone pairs of electrons in inhibitor molecules and vacant d-orbitals of metal surface[33]. CQAE possess enhanced inhibition efficiency due to the existence of delocalized π-electrons, leading to effective adsorption of the metal and also due to the high molecular weight compound in CQAE.

CONCLUSION

- At an optimum concentration of 12 v/v % the maximum efficiency attained for CQAE and CQEE are 89.45 % and 75.54 %.
- IR and GC-MS analysis confirm the presence of active species in the inhibitors.
- Electrochemical techniques affirm the inhibiting behavior of the inhibitor.
- Tafel curves suggest the mixed nature of CQAE and CQEE inhibitors.
- SEM and AFM studies provide evidence for the formation of the protective layer.
- Finally, to conclude, CQAE possess enhanced inhibition efficiency than CQEE due to the existence of active high molecular weight predominant compounds.

REFERENCES

1. P. M. Dasami, K. Parameswari and S. Chitra, *Measurement,* **69**, 195(2015), **DOI:** 10.1016/j.measurement.2015.03.025
2. M. S. Al-Otaibi, A. M. Al-Mayouf, M. Khan, A. A. Mousa and S. A. Al-Mazroa, *Arabian Journal of Chemistry,* **7 (3)**, 340(2014), **DOI:**10.1016/j.arabjc.2012.01.015
3. M. Jokar, T. Shahrabi Farahani and B. Ramezanzadeh, *Journal of Taiwan Institute of Chemical Engineers*, **63**, 436 (2016), **DOI:**10.1016/j.jtice.2016.02.027
4. M. Gopiraman, P. Sakunthala, R. Kanmani, V. Alex Ramani and N. Sulochana, *Ionics,* **17(9)**, 843(2011), **DOI:**10.1007/s11581-011-0584-9.
5. O. A. Abdullatef, *Egyptian Journal of Petroleum*, **24(4)**, 505(2015), **DOI:** 10.1016/j.ejpe.2015.03.003.
6. S. Jyothi, Y.V. Subba Rao and P.S. Samuel Ratnakumar, *Rasayan Journal of Chemistry*, **12**(2), 537 (2019), **DOI:**10.31788/RJC.2019 .122 5000
7. M. A. Deyab, M.M. Osman, A.E. Elkholyand and F.El-Taib Heakal, *RSC Advances,* **7**, 45241(2017), **DOI:** 10.1039/c7ra07979f.
8. K. K. Anupama, K. Ramya and A. Joseph, *Journal of Molecular Liquids,* **216**, 146(2016), **DOI:**10.1016/j.molliq.2016.01.019.
9. A.S. Fouda, A. Emam, R. Refat and M. Nageeb, *Journal of Analytical & Pharmaceutical Research,* **6(1)**, 1(2017), **DOI:**10.15406/japlr.2017.06.00168.
10. I.Y. Suleiman, S.A. Salihu and O.S. Emokpaire, O.C. Ogheneme and L. Shuaibu, *Portugaliae Electrochimica Acta,* **35 (3)**,143(2017), **DOI:** 10.4152/pea.201703143.
11. N. Raghavendran and J. Ishwara Bhat, *Journal of BioTribo Corrosion,* **4(1)**,1(2018), **DOI:** 10.1007/S40735-017-0112-1.
12. S. Geetu, M. Rakesh, R. Preeti, *Natural Product Research,* **21**,522(2007), **DOI:** 10.1080/14786410601130471
13. D. Jalajaa, S. Jyothi, V.R. Muruganantham and J. Mallika, *Rasayan Journal of Chemistry*, **12(2)** ,545 (2019), **DOI:**10. 31788/RJC .2019.12 24096.
14. T. A. Salman and A. B. Mohammed, *Rasayan Journal of Chemistry*, **10(3)**,815(2017), **DOI:** 10.7324/RJC.2017.1031751
15. P. Sounthari, A. Kiruthika, J. Saranya, K. Parameswari and S. Chitra, *Ecotoxicology and Environmental Safety*, **134,** 319(2016), **DOI:**10.1016/j.ecoenv.2015.08.014 .
16. P. Muthukrishnan, P. Prakash, B. Jeyaprabha and K. Shankar, *Arabian Journal of Chemistry*, (2015) **DOI:**10.1016/j.arabjc.2015.09.005.
17. V. Swarnalatha and P. Pazhanisamy, *Rasayan Journal of Chemistry*,**11(3)**,929(2018), **DOI:** 10.31788/RJC.2018.1132073
18. P. Arockiasamy, X. QueenRosarySheela, G. Thenmozhi, M. Franco, J. Wilson Sahayaraj and R.Jayasanthi, *International Journal of Corrosion*, **2014**, 1, (2014), **DOI:** 10.1155/2014/679192.

19. G. Nirmaladevi, J. Saranya, A. Kiruthika, L. O. Olasunkanmi, E. E. Ebenso and S. Chitra, *Journal of Molecular Liquids*, **232**, 9(2017), **DOI:**10.1016/j.molliq. 2017.02.054.
20. D. M. Gurudatt and N. Mohana, *Industrial and Engineering Chemistry Research*,**53**(**6**), 2092 (2014), **DOI:** 10.1021/ie402042d.
21. X. Li, S. Deng, F.M. Hui and G. Mu, *Corrosion Science*, **51(3)**, 620(2009), **DOI:** 10.1016/j.corsci.2008.12.021.
22. Y. Liu, *Colloids and Surfaces A*, **274**, 34(2006), **DOI:** 10.1016 /j.colsurfa.2005.08.029.
23. E.E. Oguzie, Y. Lia and F.H. Wang, *Electrochimica Acta*, **53(2)**, 909(2007), **DOI:**10.1016/j.electacta.2007.07.076.
24. S. Agiladevi and S. Rajendran, *Rasayan Journal of Chemistry*, **12(1)**, 22(2019), **DOI:** 10.31788/RJC.2019.1215037.
25. T. Deepa and C. Thangavelu, *Rasayan Journal of Chemistry*, **10(2)**, 584 (2017), **DOI:** 10.7324/RJC.2017.1021550.
26. S. Jyothi, K. Rathidevi, D. Jalajaa and P.S. Samuel Ratnakumar, *Rasayan Journal of Chemistry*, **12(1)**, 272 (2019), **DOI:**10.31788/RJC.2019.1214097
27. N. Anusuya, J. Saranya, P. Sounthari, A. Zarrouk and S. Chitra, *Journal of Molecular Liquids*, **225**, 406 (2017), **DOI:** 10.1016/j.molliq.2016.11. 015.
28. S. Jyothi and K. Rathidevi, *Rasayan Journal of Chemistry*, **10(4)**, 1253(2017), **DOI:** 10.7324/RJC.2017.1041924.
29. P. Muthukrishnan, B. Jeyaprabha and P.Prakash, *Arabian Journal of Chemistry*, **10**, S2343 (2017), **DOI:**10.1016/j.arabjc.2013.08.011.
30. M. Prabakaran, S.H. Kim, Y. Takoh, V. Raj and I. M. Chung, *Journal of Industrial and Engineering Chemistry*, **45**, 380 (2017), **DOI:** 10.1016 /j.jiec.2016.10.006.
31. X. Li, S. Deng and H. Fu, *Corrosion Science*, **62**, 163(2012), **DOI:**10.1016/j.corsci.2012.05.008
32. P.M. Krishnegowda, V.T. Venkatesha, P.M. Krishnegowda and S.B.Shivayogiraju, *Industrial & Engineering Chemistry Research*, **52(2)**,722(2013), **DOI:**10.1021/ie3018862.
33. A. Lecante, F. Robert, P.A. Blandinieres and C. Roos, *Current Applied Physics*, **11(3)**, 714 (2011) **DOI:**10.1016/j.cap.2010.11.038.

[RJC-5195/2019]